Available online at www.sciencedirect.com
ScienceDirect
Biochemical and Biophysical Research Communications 348 (2006) 393–399
BBRC
www.elsevier.com/locate/ybbrc

Overexpression of adenine nucleotide translocase reduces Ca^{2+} signal transmission between the ER and mitochondria

Mariusz R. Wieckowski [a,b], György Szabadkai [a], Michał Wasilewski [b], Paolo Pinton [a], Jerzy Duszyński [b], Rosario Rizzuto [a,*]

[a] Department of Experimental and Diagnostic Medicine, Section of General Pathology, Interdisciplinary Center for the Study of Inflammation (ICSI) and Emilia Romagna Laboratory for Genomics and Biotechnology (ER-Gentech), University of Ferrara, Via Borsari 46, I-44100 Ferrara, Italy
[b] Department of Cellular Biochemistry, Nencki Institute of Experimental Biology, Polish Academy of Sciences, Pasteur 3, 02-093 Warsaw, Poland

Received 3 July 2006
Available online 25 July 2006

Abstract

The adenine nucleotide translocase (ANT), besides transferring ATP from the mitochondrial matrix to the rest of the cell, has also been proposed to be involved in mitochondrial permeability transition (MPT), and accordingly in mitochondrial Ca^{2+} homeostasis. In order to assess the role of ANT in Ca^{2+} signal transmission from the endoplasmic reticulum (ER) to mitochondria, we overexpressed the various ANT isoforms and measured the matrix $[Ca^{2+}]$ ($[Ca^{2+}]_m$) increases evoked by stimulation with IP_3-dependent agonists. ANT overexpression reduced the amplitude of the $[Ca^{2+}]_m$ peak following Ca^{2+} release, an effect that was markedly greater for ANT-1 and ANT-3 isoforms than for ANT-2. Three further observations might explain these findings. First, the effect was partially reversed by treating the cells with cyclosporine A, suggesting the involvement of MPT. Second, the effect was paralleled by alterations of the 3D structure of the mitochondria. Finally, ANT-1 and ANT-3 overexpression also caused a reduction of ER Ca^{2+} loading that caused a marginal decrease in the cytosolic Ca^{2+} responses. Overall, these data provide evidence for the involvement of ANT-1 and ANT-3 in the induction of MPT and indicate the relevance of this phenomenon in ER–mitochondria Ca^{2+} transfer.

Keywords: Mitochondria; Adenine nucleotide translocase; Permeability transition pore; Calcium homeostasis

The primary role of the ADP/ATP translocator (ANT) is the exchange of ADP and ATP across the inner mitochondrial membrane (IMM). Following the molecular identification of the most abundant ANT isoform, member 4 of the solute carrier family 25 proteins [1], recently the presence of different ANT isoforms in various tissues has been reported. In rat and mouse, ANT-1 is mainly present in skeletal muscle, heart, kidney, and the brain, whereas the ANT-2 isotype is predominant in the tissues with regenerative capacity [1]. ANT-3 was shown to be present in small amount in virtually all tissues [1,2]. However, despite the tissue specific predominance of the different subtypes, ANT-1, ANT-2, and ANT-3 appear to co-exist within the mitochondria of the same cell, with a different distribution. Indeed, it was shown that the peripheral inner mitochondrial membrane contains all three isoforms of ANT, whereas the ANT-2 isoform is present exclusively in cristae membranes [3]. This particular distribution also suggested specific functions of the ANT isoforms [4]. Indeed, parallel to its characterization as adenine nucleotide exchanger, extensive studies have shown that ANT participates in the development of mitochondrial permeability transition (MPT).

MPT is characterized by the opening of a non-specific large conductance pore of the inner and outer mitochondrial membranes (IMM and OMM, respectively) termed as mitochondrial permeability transition pore (MPTP). MPT can be induced by the combination of high mitochondrial

* Corresponding author. Fax: +39 0532 247278.
E-mail address: r.rizzuto@unife.it (R. Rizzuto).

0006-291X/$ - see front matter © 2006 Elsevier Inc. All rights reserved.
doi:10.1016/j.bbrc.2006.07.072

$[Ca^{2+}]$ ($[Ca^{2+}]_m$), oxidative stress, ATP depletion, and high inorganic phosphate [5]. While the exact molecular nature of the MPTP is still debated, it is generally proposed that the core structure of the pore includes the voltage-dependent anion channel (VDAC) of the OMM, the ANT of the IMM, and cyclophilin-D (Cyp-D) of the mitochondrial matrix. However, the issue is far from being settled, as permeability transition was shown to occur in cells devoid of all three isoforms [6]. It was also suggested that members of the Bcl-2 family proteins, the 'peripheral type' benzodiazepine receptor, and hexokinase interact with the MPTP [7].

Cyp-D is the target of cyclosporine A (CsA), the best characterized inhibitor of the MPTP [8], and it mediates the Ca^{2+}-dependent MPTP open/closed transitions by reversible binding to ANT. Importantly, ANT-1 and ANT-3 display higher affinity for Cyp-D than ANT-2 [3], suggesting a more specific role in MPT induction. Upon opening of the PTP, increased permeability of the mitochondrial membranes leads to collapse of the mitochondrial membrane potential ($\Delta\psi_m$). In isolated mitochondria, MPT induces osmotic mitochondrial swelling, breakdown of the OMM, and release of several apoptotic factors, such as AIF (apoptosis-inducing factor) [9], cytochrome *c* [10], and Smac/Diablo [11,12]. Whether this mechanism can also operate in intact cells is still a matter of debate, but Bauer et al. described that overexpression of ANT-1 but not ANT-2 induced apoptosis in several cell lines even if its ATP/ADP exchanger activity is impaired by point mutations [13]. In addition, Zamora et al. found that overexpression of ANT-3 also leads to induction of apoptosis [14].

Mitochondria, due to the membrane potential ($\Delta\psi_m$), negative inside, generated by the respiratory chain, readily accumulate Ca^{2+} during cell stimulation. This uptake is mediated by a low affinity ($K_d > 10\ \mu M$) Ca^{2+} activated calcium channel (the mitochondrial Ca^{2+} uniporter, MCU), localized in the IMM. Mitochondria are highly responsive to agonist stimulation because they are closely positioned to IP_3-gated Ca^{2+} release channels (IP_3 receptors, IP_3R) of the ER [15]. Upon opening of the IP_3R, the locally formed high Ca^{2+} concentration microdomain is transferred through the OMM voltage-dependent anion channel (VDAC), and consequently activates the MCU of the IMM. Ca^{2+} is then released from the mitochondria through Na^+/Ca^{2+} and H^+/Ca^{2+} exchange mechanisms, the molecular nature of which is still unknown. Moderate calcium uptake into the mitochondrial matrix activates metabolic activity [16], while excessive Ca^{2+} load and/or the effect of other mediators such as ceramide induces mitochondria apoptosis probably through induction of MPT. In addition to the above-described mitochondrial Ca^{2+} transport mechanisms, recently it has been shown that MPT may also participate in mitochondrial Ca^{2+} homeostasis in two different ways. First, Ca^{2+} induced MPT leads to Ca^{2+} extrusion from the mitochondrial matrix, which in particular systems may serve as an amplification loop for Ca^{2+} induced Ca^{2+} release from the ER/sarcoplasmic reticulum Ca^{2+} stores. In addition, reversible, flickering MPT pore opening was proposed to finely tune $\Delta\psi_m$, thus determining the driving force for Ca^{2+} uptake and free radicals production [17]. Additionally, in our previous paper we showed that also mitochondrial shape can affect organelle Ca^{2+} uptake, by controlling the diffusion to the whole network of Ca^{2+} entering mitochondria at the sites of contact with the ER. Probably it can be due to changes of mitochondria interaction with the ER and plasmamembrane. Overexpression of Drp-1 causes division of the mitochondrial network and blocks intraorganellar Ca^{2+} waves [18]. Frieden et al. demonstrated that the fragmented perinuclear mitochondrial population slower accumulates Ca^{2+} from extracellular sources even if the capability of mitochondria to take up Ca^{2+} released from the ER remain unaltered [19,20]. Moreover, PGC-1α selectively reduced mitochondrial Ca^{2+} responses to cell stimulation by reducing the efficacy of mitochondrial Ca^{2+} uptake sites and increasing organelle volume [21].

Based on the proposed interaction between the putative MPT pore component ANT and Ca^{2+} signaling we aimed to characterize the role of the three ANT isoforms (ANT-1, ANT-2, and ANT-3) in mitochondrial Ca^{2+} uptake. Thus, we used targeted aequorin probes to monitor $[Ca^{2+}]$ changes in cells overexpressing these particular ANT isoforms. In parallel using confocal microscopy we assessed changes in mitochondrial morphology and their interaction with the ER.

Materials and methods

Cell culture and transfection. HeLa cells were grown in Dulbecco's modified Eagle's medium (DMEM), supplemented with 10% fetal calf serum (FCS), in 75 cm^2 Falcon flasks. For aequorin measurement, before transfection, cells were seeded onto 13 mm glass coverslips and allowed to grow to 50% confluence. At this stage, transfection with 4 μg of DNA (control cells: 3 μg mtGFP + 1 μg AEQ; ANT overexpressing cells: 3 μg ANT + 1 μg AEQ) was carried out as previously described [30] and aequorin measurements were performed 36 h after transfection. For mitochondrial structure and mitochondrial membrane potential cells (seeded onto 24 mm coverslips) were transfected with 2 μg mtGFP and 6 mg ANT expressing vectors. For mitochondrial and ER structure cells (seeded onto 24 mm coverslips) were transfected with 2 μg ERGFP and 6 mg ANT expressing vectors. Cells were transfected with the calcium phosphate method as described before [22]. All cDNAs were in pcDNA3 plasmid. Green fluorescent protein and aequorin selectively targeted to organelle of interest (ERGFP, cytAEQ, mtAEQ, and ERAEQ) were previously engineered in laboratory of Professor R. Rizzuto. All ANT cDNAs were obtained from Professor G. Kroemer.

Estimation of the overexpression level of ANT-1, ANT-2, and ANT-3 isoform in HeLa cells. The efficiency of the overexpression of three isoforms of ANT was analyzed by Western blot analysis. HeLa cells plated in 10-cm petri dishes were transfected with 30 μg of each plasmid (ANT-1, ANT-2, and ANT-3). The cells were harvested, 36 h after transfection, by trypsinization and centrifuged at 600*g* for 10 min. The cell pellet was washed twice in PBS and resuspended in 2 ml of buffer A (sucrose 250 mM, Hepes 20 mM, pH 7.4, KCl 10 mM, EDTA 1 mM, $MgCl_2$ 1 mM, and DTT 1 mM) supplemented with 1 × protease inhibitor cocktail (Sigma–Aldrich). After chilling on ice for 30 min with frequent tapping, cells were lysed with 50 strokes of glass Dounce homogenizer (this lysate corresponds to total proteins). For detection of ANT expression whole cell lysate was prepared using standard protocol. Protein was quantified using

Bradford method (Bio-Rad). Forty micrograms of total protein was separated by SDS–PAGE 10%. Western blotting was performed using polyclonal ANT antibody (Santa Cruz Biotechnology) diluted 1:1000 and monoclonal β-tubulin antibody (Santa Cruz) diluted 1:5000. After hybridization with peroxidase (HRP)-conjugated secondary antibody, the signal was revealed using ECL Plus Western blot detection reagent (Amersham Pharmacia Biotech).

Aequorin measurements. For cytosolic aequorin (cytAEQ) and mitochondrial aequorin (mtAEQ) the coverslips with the cells were incubated with 5 μM coelenterazine for 1–2 h in DMEM supplemented with 1% FCS and then transferred to the perfusion chamber. For reconstitution with the aequorin chimera targeted to the ER (erAEQ), the luminal $[Ca^{2+}]$ of this compartment was first reduced. This was obtained by incubating the cells for 1 h at 4 °C in Krebs–Ringer modified buffer (KRB) (125 mM NaCl, 5 mM KCl, 1 mM Na_3PO_4, 1 mM $MgSO_4$, 5.5 mM glucose, and 20 mM Hepes, pH 7.4, 37 °C) supplemented with coelenterazine 5 μM, the Ca^{2+} ionophore ionomycin, and 600 μM EGTA. After this incubation the cells were extensively washed with KRB supplemented with 2% BSA (bovine serum albumin) and 1 mM EGTA, then aequorin reconstitution was carried out as described above.

All aequorin measurements were carried out in KRB. Agonists and other drugs were added to the same medium, as specified in the figure legends. The experiments were terminated by lysing cells with 100 μM digitonin in a hypotonic Ca^{2+}-rich solution (10 mM $CaCl_2$ in H_2O), thus discharging the remaining aequorin pool. The light signal was collected and calibrated into $[Ca^{2+}]$ values as previously described [22–24]. The aequorin luminescence data were calibrated off-line into $[Ca^{2+}]$ values, using a computer algorithm based on the Ca^{2+} response curve of wild-type and mutant aequorins, as previously described [23,24]. All the results are expressed as means ± standard error (SE).

Measurements of mitochondrial membrane potential. $\Delta\psi_m$ was measured by loading cells with tetramethyl-rhodamine-methylester (TMRM, 10 nM, 30 min, 37 °C) [25]. TMRM fluorescence was detected on Zeiss confocal microscope (LSM 510 equipped with a plan-Apochromat 63× oil immersion objective) or iCys Scanning Microscope. The 543 nm excitation wavelength was provided by a HeNe laser source. Signal was collected as total emission > 570 nm. To distinguish control from the ANT/mtGFP transfected cells, green emission was collected as emission from the range 505 to 535 nm. To accurately measure fluorescence emission from the entire mitochondrial network, a maximal 3D projection of confocal images on the *z*-axis was obtained by means of the LSM software (Zeiss). Fluorescence was quantified and corrected for background emission with the cell imaging software Metamorph 2.3 (Universal Imaging Corporation, PA, USA).

Analysis of mitochondrial and endoplasmic reticulum morphology. Cells were transiently transfected with ERGFP (control) and ERGFP cotransfected with one of ANT isoforms (ANT-1 or ANT-2 or ANT-3). Transfected cells were loaded at the same time with 20 nM MitoTracker Deep-Red to study mitochondrial structure. Images were acquired with a LSM 510 Zeiss confocal microscope. To achieve a higher resolution of the mitochondrial and ER network, images were analyzed with an algorithm for 3D reconstruction developed from the Biomedical Imaging Group of the University of Massachusetts (Worcester, MA, USA) based on point spread function analysis [26]. All experiments were performed at 37 °C in the modified KRB solution. For the colocalization analysis of fluorescence signals the data analysis and visualization environment (DAVE) software was used to visualize images in three dimensions, to superimpose them, and to determine the extent to which they coincided [27].

Results

Mitochondrial Ca^{2+} uptake is markedly inhibited by overexpression of ANT-1 and ANT-3 isoforms

In order to study the role of ANT in mitochondrial calcium handling we overexpressed ANT-1, ANT-2, and ANT-3 in HeLa cells and analyzed calcium homeostasis at different subcellular compartments using the recombinant aequorin technique [23,28,29]. First, HeLa cells were transfected either with a mitochondria targeted mutated low affinity aequorin chimera alone (mtAEQmut control) or co-transfected with the three ANT isoforms and mtAEQmut together (ANT-1, ANT-2, and ANT-3, respectively). As confirmed by Western blot analysis, the level of expression of the particular isoforms was practically identical (Fig. 1C). Both in control and ANT-transfected HeLa cells, application of 100 μM histamine, through $G_{q/o}$ coupled receptors, caused a rapid increase of mitochondrial Ca^{2+} concentration ($[Ca^{2+}]_m$), following IP_3 induced Ca^{2+} release from the endoplasmic reticulum Ca^{2+} store (Fig. 1A). However, overexpression of the ANT-1 and ANT-3 isoforms induced a large decrease (~40%) of mitochondria calcium uptake. In contrast, in the ANT-2 overexpressing cells, the mitochondrial Ca^{2+} transient was much less reduced (~20%).

This subtype specific effect of ANT overexpression led us to consider the possibility that the ANT-1 and ANT-3 isoforms might affect mitochondrial calcium uptake by the formation of new MPT pores. To verify this hypothesis, control and ANT transfected cells were treated with 300 nM cyclosporin A (CsA) for 2 h before calcium measurement to inhibit MPTP opening during the experiment. As shown in Fig. 1B, inhibition of PTP opening by CsA partially abolished the inhibitory effect of ANT-1 and ANT-3 mediated inhibition of the mitochondrial Ca^{2+} response, arguing for a role of MPT in the effect of the overexpression.

Ca^{2+} release from the endoplasmic reticulum is slightly modified by ANT-3 overexpression

Next, we investigated whether the observed mitochondrial calcium changes ($[Ca^{2+}]_m$) (Fig. 1A and B) were corresponding to alterations of cytosolic and ER calcium concentration ($[Ca^{2+}]_c$, $[Ca^{2+}]_{ER}$). HeLa cells were transfected either with the specific aequorin chimeras—cytosolic or ER alone (cytAEQ and erAEQmut, controls) or co-transfected with each ANT isoforms and the cytAEQ or erAEQmut probe. As shown in Fig. 2A, the cytosolic calcium transients evoked by the addition of 100 μM histamine are comparable in control and ANT-1, ANT-2 transfected HeLa cells. In ANT-3 transfected cells a small but reproducible reduction of cytosolic response was observed.

Although the key parameter for mitochondrial Ca^{2+} uptake (the $[Ca^{2+}]_c$ transient) was practically unaffected, we analyzed the ER calcium content in control and ANT transfected cells. This parameter, due to the intimate connections between the ER and mitochondria, may have a greater impact on mitochondrial calcium uptake than $[Ca^{2+}]_c$, and reduced mitochondrial calcium uptake in ANT-1 and ANT-3 transfected cells could be a result of the lower ER $[Ca^{2+}]$ ($[Ca^{2+}]_{ER}$) levels. Indeed, Brini and co-workers showed that the mitochondrial Ca^{2+} responses

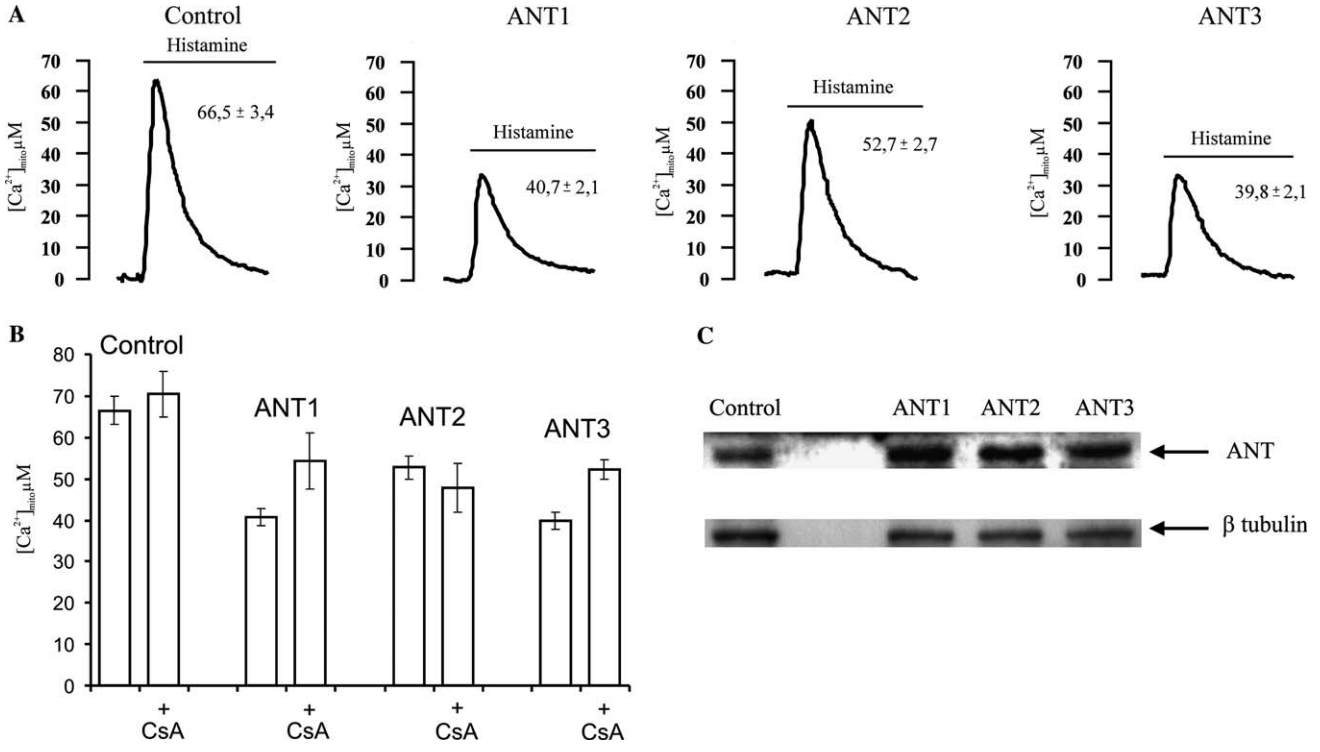

Fig. 1. Mitochondrial Ca^{2+} homeostasis in control and ANT-overexpressing HeLa cells. Effect of cyclosporine A on mitochondrial Ca^{2+} uptake. (A) Parallel batches of HeLa cells where co-transfected either with the mitochondrial AEQ chimera (mtAeq) and the different ANT isoforms, or transfected with the mtAEQ chimera alone (control). Where indicated, cells were challenged with 100 µM histamine. Thirty-six hours after transfection, the measurement of AEQ luminescence was carried out and calibrated into $[Ca^{2+}]$ values as described in Materials and methods. In this, and in the following aequorin experiments, the traces are representative of at least five experiments, which gave similar results. (B) Two hours before mitochondrial calcium uptake measurements, cells were treated with 300 nM cyclosporine A (CsA). (C) Immunoblotting of control and ANT transfected HeLa cells. Overexpression level of ANT-1, ANT-2, and ANT-3 estimated with polyclonal anti-ANT antibodies.

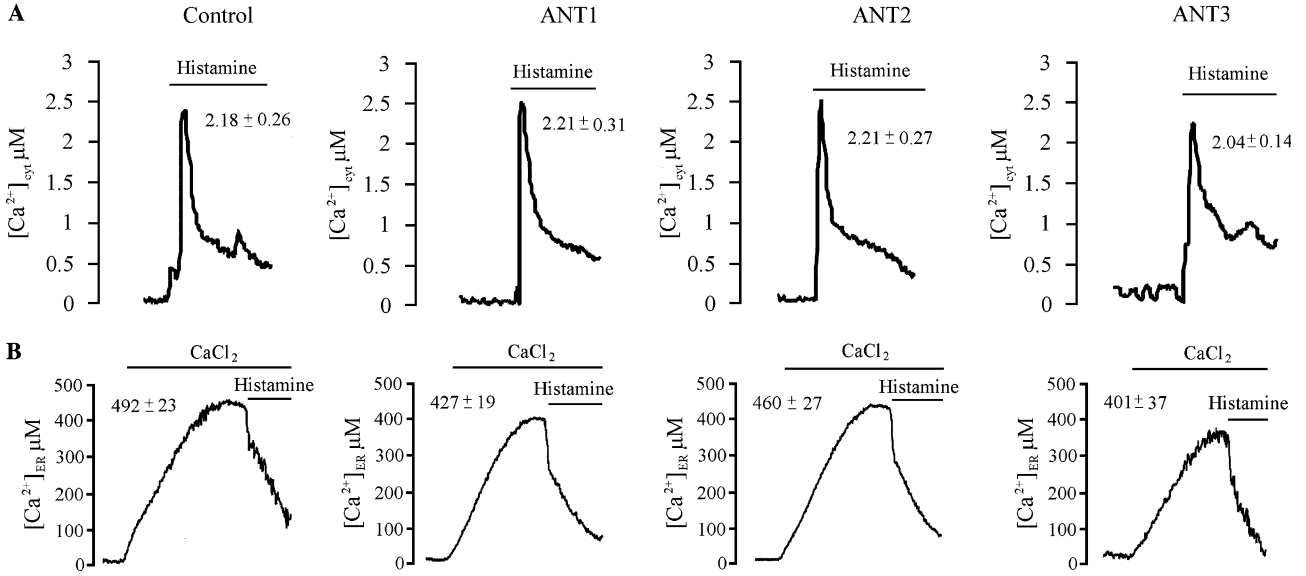

Fig. 2. Ca^{2+} homeostasis in cytosol and lumen of ER in control and ANT-overexpressing HeLa cells. HeLa cells were cotransfected either with the appropriate AEQ chimera (A) cyt Aeq, (B) ERAeq and different ANT isoforms, or transfected with the AEQ chimera alone (control). Where indicated, the cells where challenged with 100 µM histamine.

correlate to the state of filling of the Ca^{2+} stores and the rate and extent of Ca^{2+} release rather than to the $[Ca^{2+}]$ rise detected in the bulk cytosol [30]. Fig. 2B shows the effect of ANT-1, ANT-2, and ANT-3 overexpression on the steady state $[Ca^{2+}]_{ER}$ level and the kinetics of Ca^{2+} release, following histamine stimulation. Importantly, we

observed a small reduction of steady state $[Ca^{2+}]_{ER}$ level in both ANT-1 and ANT-3 transfected cells, which thus can be responsible for the reduced $[Ca^{2+}]_m$ response in these cells. This finding might explain why CsA treatment does not completely recover mitochondrial Ca^{2+} response to the control level.

Selective modification of mitochondrial structure might contribute to the reduction of mitochondrial Ca^{2+} uptake by upregulation of ANT-1 and ANT-3

Since alterations in mitochondrial metabolism can influence organelle structure, and we showed recently forced division of the tubular mitochondrial network results in decreased $[Ca^{2+}]_m$ responses [18], in the next set of experiments we investigated whether the ANT overexpression induces modifications of the mitochondrial and ER structure. In particular, we examined whether the $[Ca^{2+}]_m$ and $[Ca^{2+}]_{ER}$ changes observed in ANT-1 and ANT-3 transfected cells were paralleled by alterations of mitochondrial and ER morphology. HeLa cells were transfected with ER targeted GFP (in order to visualize endoplasmic reticulum, controls, Fig. 3), or co-transfected with ER targeted GFP and each ANT isoform (ANT-1, ANT-2, ANT-3 overexpressing cells). The mitochondrial structure was evaluated by loading the cells with the MitoTracker Deep-Red dye, allowing the parallel visualization of both organelles by confocal microscopy without crosstalk between the fluorescent signals. As shown in Fig. 3, mitochondria in control cells form a continuous intracellular network (in red), interrelated with the more dense and thin ER structure (in green). Analysis of images showed that the ER morphology was not affected by overexpression of any of ANT isoforms, while the mitochondrial network was fragmented in ANT-1 and ANT-3 transfected cells, as compared to controls. The most striking fragmentation was observed in ANT-3 transfected cells. Despite this change in the mitochondrial morphology, further colocalization analysis reveals no difference between number of mitochondria colocalizing voxels in ANT-1 (5.28 ± 0.93), ANT-2 (6.12 ± 0.72), and ANT-3 overexpressing cells (6.01 ± 0.37), compared to control cells (5.75 ± 0.62). This result suggests that there is no difference in the number of ER–mitochondria contacts between control and ANT transfected cells.

As we have previously shown, fragmentation of the mitochondrial network without the modification of ER–mitochondria contact leads to limited Ca^{2+} diffusion in the mitochondrial network, a heterogeneous Ca^{2+} response, and thus, an overall reduction of the mitochondrial Ca^{2+} load [18]. Thus, we concluded that the observed structural modification of the mitochondrial network in ANT-1 and ANT-3 expressing cells might result in reduction of mitochondrial Ca^{2+} uptake, adding a further mechanism for the reduction of ER Ca^{2+} content and mitochondrial depolarization.

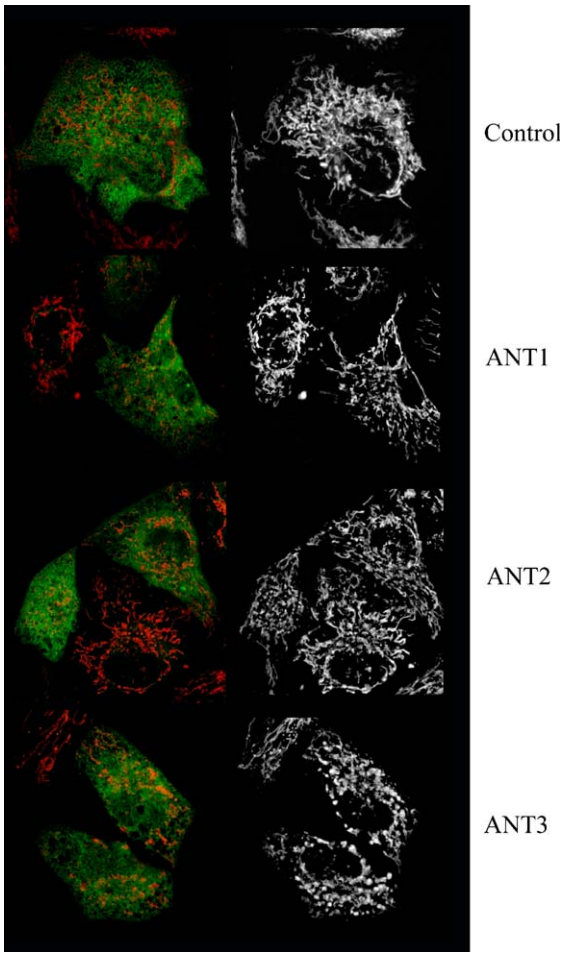

Fig. 3. Mitochondrial and ER morphology in control and ANT overexpressing cells. Confocal images of control and ANT transfected cells overexpressing ER-GFP and loaded with 20 nM MitoTracker Deep-Red. Mitochondria (red) in control and ANT transfected cells were visualized by loading cells with MitoTracker Deep-Red. ER (green) in a control and ANT transfected cells was visualized by overexpression of ER-GFP (see Materials and methods for experimental details). (For interpretation of the references to color in this figure legend, the reader is referred to the web version of this paper.)

Discussion

In the last years, several lines of evidence demonstrated a crucial role for mitochondria in cellular Ca^{2+} signaling. First, drastic inhibition of mitochondrial Ca^{2+} uptake by mitochondrial uncouplers was shown to change the kinetic of global $[Ca^{2+}]_c$ transients, proving a buffering role of the organelle [31]. In addition, using high resolution light and electron microscopy, some regions of ER were shown to form close contacts with mitochondria [32], giving rise to a mutual regulation of ER Ca^{2+} release and mitochondrial Ca^{2+} uptake. The MCU, while its molecular nature is still not yet identified, was recently characterized by electrophysiological means [33]. In contrast, much less is known about the intrinsic regulation of mitochondrial Ca^{2+} uptake by protein components of the inner and outer membrane. We have recently shown that the OMM channel VDAC-1 underlies the Ca^{2+} permeability of the OMM,

transferring high Ca^{2+} microdomains from the mouth of the IP_3R to the intermembrane space [18,27]. In addition, microtubule driven mitochondrial dynamics [34], large GTPase driven fusion/fission of the mitochondrial network [18,35] as well as PGC-1α induced mitochondrial biogenesis was also shown to modify the extent of mitochondrial Ca^{2+} load.

Here, we present results which open a new aspect of the regulation of mitochondrial Ca^{2+} uptake. Our work dissected the pleiotropic effect of upregulation of specific ANT isoforms. The results indicate that overexpression of different ANT isoforms induces specific and different alterations in calcium homeostasis. Only ANT-1 and ANT-3 isoforms, that are postulated to be integral part of PTP, induced dramatic decrease of mitochondria calcium uptake. In contrast to control and ANT-2 transfected cells, inhibition of PTP in ANT-1 and ANT-3 transfected cells causes a significant increase of mitochondrial Ca^{2+} response. Moreover, we postulate that increased number of MPT pores (possible formed by additional ANT molecules) present in mitochondria of cells overexpressing ANT-1 and ANT-3 is able to modulate the mitochondrial Ca^{2+} response without significant alterations in the global cellular calcium homeostasis.

The sensitivity of the ANT-1 and ANT-3 effect to MPT blockers can be explained by the help of the recent theory of the role of MPT in maintaining $\Delta\psi_m$, i.e., to prevent extreme hyperpolarization of the IMM which causes increase of free radical production by mitochondria [17]. Reversible flickering of the MPT pore between open and closed states was repetitively shown under different experimental conditions [36,37]. Such opening of the pore might lead to a localized depolarization in the mitochondrial network, which, however, does not spread to the whole network, but rather is quickly compensated by the H^+ pumping activity of the electron transport chain. Upregulation of the pore component ANT-1 and ANT-3 might augment the frequency of these events, without leading to a general depolarization of the whole mitochondrial network. In these ANT-1 and ANT-3 transfected cells, we have not found any significant shift in $\Delta\psi_m$ as measured by TMRM on the Zeiss Confocal Microscope and iCys Scanning Microscope (data not shown). This does not exclude the occurrence of local flickering episodes due to their transient duration [36,37]. Moreover, upregulation of the number of MPT pores in these cells is expected to confer also increased Ca^{2+}-sensitivity of MPT, thus leading to a more profound $\Delta\psi_m$ loss at the sites of Ca^{2+} uptake, thus, decreasing the driving force for Ca^{2+} influx during cell stimulation, explaining the observed reduction of mitochondrial Ca^{2+} uptake.

In addition, local provision of ATP to SERCA pumps (the tight bioenergetic coupling underlying efficient Ca^{2+} loading in the ER) could be partly impaired. The consequent modest reduction in ER filling, while affecting very modestly cytosolic [Ca^{2+}] increases, could participate in reducing the efficiency of ER–mitochondria Ca^{2+} coupling.

Interestingly, apart from the CsA-, i.e., MPT-dependent reduction of the mitochondrial Ca^{2+} uptake, we observed an additional component, remaining after CsA addition. One clue to explain this further reduction might come from the observation that ANT-1 and ANT-3 overexpressing cells displayed a drastically fragmented mitochondrial network. Importantly, this fragmentation was similar to the fragmentation observed previously by overexpressing the mitochondrial fission component Drp-1 [18], in the sense that the fragmented mitochondrial particles preserved their close connection to the ER. Analysis of the spreading of Ca^{2+} waves from these sites (hot spots) led to the conclusion that fragmentation leads to blockade of complete uploading of the mitochondrial network, i.e., to the reduction of the overall mitochondrial Ca^{2+} uptake. The mechanism by which ANT-1 and ANT-3 overexpression and/or MPTP upregulation leads to mitochondrial fragmentation is unknown, but in this respect it is important to note that the efficient fusion of the IMM, a preserved $\Delta\psi_m$, was shown to be necessary.

In conclusion, our work showed a partially MPTP dependent inhibition of the overall mitochondrial Ca^{2+} uptake following overexpression of the ANT-1 and ANT-3 isoforms, which most probably reflects local loss of $\Delta\psi_m$. Further experiments are necessary to reveal the sub-mitochondrial dynamics of $\Delta\psi_m$ changes and its effect on intramitochondrial Ca^{2+} waves, as well as to describe the mechanism by which these changes lead to the fragmentation of the mitochondrial network.

Acknowledgments

We thank the KBN—Poland (Grant Nos. 3 P04A 04123), the Italian University Ministry (MURST), Telethon—Italy (Grant Nos. GGP05284 and GTF02013), the Italian Association for Cancer Research (AIRC), the Italian Space Agency (ASI), EU (fondi strutturali Obiettivo 2), and the PRRIITT program of the Emilia Romagna Region for financial support. M.R.W. was the recipient of FEBS long-term fellowship. We thank Prof. G. Kroemer for providing the ANT cDNAs.

References

[1] A. Doerner, M. Pauschinger, A. Badorff, M. Noutsias, S. Giessen, K. Schulze, J. Bilger, U. Rauch, H.P. Schultheiss, Tissue-specific transcription pattern of the adenine nucleotide translocase isoforms in humans, FEBS Lett. 414 (1997) 258–262.

[2] G. Stepien, A. Torroni, A.B. Chung, J.A. Hodge, D.C. Wallace, Differential expression of adenine nucleotide translocator isoforms in mammalian tissues and during muscle cell differentiation, J. Biol. Chem. 267 (1992) 14592–14597.

[3] M.Y. Vyssokikh, A. Katz, A. Rueck, C. Wuensch, A. Dorner, D.B. Zorov, D. Brdiczka, Adenine nucleotide translocator isoforms 1 and 2 are differently distributed in the mitochondrial inner membrane and have distinct affinities to cyclophilin D, Biochem. J. 358 (2001) 349–358.

[4] M. Klingenberg, The ADP-ATP translocation in mitochondria, a membrane potential controlled transport, J. Membr. Biol. 56 (1980) 97–105.

[5] P. Bernardi, R. Colonna, P. Costantini, O. Eriksson, E. Fontaine, F. Ichas, S. Massari, A. Nicolli, V. Petronilli, L. Scorrano, The mitochondrial permeability transition, Biofactors 8 (1998) 273–281.
[6] J.E. Kokoszka, K.G. Waymire, S.E. Levy, J.E. Sligh, J. Cai, D.P. Jones, G.R. MacGregor, D.C. Wallace, The ADP/ATP translocator is not essential for the mitochondrial permeability transition pore, Nature 427 (2004) 461–465.
[7] D.R. Green, J.C. Reed, Mitochondria and apoptosis, Science 281 (1998) 1309–1312.
[8] V. Petronilli, A. Nicolli, P. Costantini, R. Colonna, P. Bernardi, Regulation of the permeability transition pore, a voltage-dependent mitochondrial channel inhibited by cyclosporin A, Biochim. Biophys. Acta 1187 (1994) 255–259.
[9] S.A. Susin, H.K. Lorenzo, N. Zamzami, I. Marzo, B.E. Snow, G.M. Brothers, J. Mangion, E. Jacotot, P. Costantini, M. Loeffler, N. Larochette, D.R. Goodlett, R. Aebersold, D.P. Siderovski, J.M. Penninger, G. Kroemer, Molecular characterization of mitochondrial apoptosis-inducing factor, Nature 397 (1999) 441–446.
[10] R.M. Kluck, E. Bossy-Wetzel, D.R. Green, D.D. Newmeyer, The release of cytochrome *c* from mitochondria: a primary site for Bcl-2 regulation of apoptosis, Science 275 (1997) 1132–1136.
[11] C. Du, M. Fang, Y. Li, L. Li, X. Wang, Smac, a mitochondrial protein that promotes cytochrome *c*-dependent caspase activation by eliminating IAP inhibition, Cell 102 (2000) 33–42.
[12] A.M. Verhagen, P.G. Ekert, M. Pakusch, J. Silke, L.M. Connolly, G.E. Reid, R.L. Moritz, R.J. Simpson, D.L. Vaux, Identification of DIABLO, a mammalian protein that promotes apoptosis by binding to and antagonizing IAP proteins, Cell 102 (2000) 43–53.
[13] M.K. Bauer, A. Schubert, O. Rocks, S. Grimm, Adenine nucleotide translocase-1, a component of the permeability transition pore, can dominantly induce apoptosis, J. Cell Biol. 147 (1999) 1493–1502.
[14] M. Zamora, M. Granell, T. Mampel, O. Vinas, Adenine nucleotide translocase 3 (ANT3) overexpression induces apoptosis in cultured cells, FEBS Lett. 563 (2004) 155–160.
[15] R. Rizzuto, P. Pinton, W. Carrington, F.S. Fay, K.E. Fogarty, L.M. Lifshitz, R.A. Tuft, T. Pozzan, Close contacts with the endoplasmic reticulum as determinants of mitochondrial Ca^{2+} responses, Science 280 (1998) 1763–1766.
[16] L.S. Jouaville, P. Pinton, C. Bastianutto, G.A. Rutter, R. Rizzuto, Regulation of mitochondrial ATP synthesis by calcium: evidence for a long-term metabolic priming, Proc. Natl. Acad. Sci. USA 96 (1999) 13807–13812.
[17] S.S. Korshunov, V.P. Skulachev, A.A. Starkov, High protonic potential actuates a mechanism of production of reactive oxygen species in mitochondria, FEBS Lett. 416 (1997) 5–18.
[18] G. Szabadkai, A.M. Simoni, M. Chami, M.R. Wieckowski, R.J. Youle, R. Rizzuto, Drp-1 dependent division of the mitochondrial network blocks intraorganellar Ca^{2+} waves and protects against Ca^{2+} mediated apoptosis, Mol. Cell 16 (2004) 59–68.
[19] M. Frieden, D. James, C. Castelbou, A. Danckaert, J.C. Martinou, N. Demaurex, Ca^{2+} homeostasis during mitochondrial fragmentation and perinuclear clustering induced by hFis1, J. Biol. Chem. 279 (2004) 22704–22714.
[20] M. Frieden, S. Arnaudeau, C. Castelbou, N. Demaurex, Subplasmalemmal mitochondria modulate the activity of plasma membrane Ca^{2+}-ATPases, J. Biol. Chem. 280 (2005) 43198–43208.
[21] K. Bianchi, G. Vandecasteele, C. Carli, A. Romagnoli, G. Szabadkai, R. Rizzuto, Regulation of Ca^{2+} signalling and Ca^{2+}-mediated cell death by the transcriptional coactivator PGC-1alpha, Cell Death Differ. 13 (2006) 586–596.
[22] R. Rizzuto, M. Brini, C. Bastianutto, R. Marsault, T. Pozzan, Photoprotein-mediated measurement of calcium ion concentration in mitochondria of living cells, Methods Enzymol. 260 (1995) 417–428.
[23] M. Brini, R. Marsault, C. Bastianutto, J. Alvarez, T. Pozzan, R. Rizzuto, Transfected aequorin in the measurement of cytosolic Ca^{2+} concentration ($[Ca^{2+}]c$). A critical evaluation, J. Biol. Chem. 270 (1995) 9896–9903.
[24] M.J. Barrero, M. Montero, J. Alvarez, Dynamics of $[Ca^{2+}]$ in the endoplasmic reticulum and cytoplasm of intact HeLa cells. A comparative study, J. Biol. Chem. 272 (1997) 27694–27699.
[25] R.C. Scaduto, L.W. Grotyohann, Measurement of mitochondrial membrane potential using fluorescent rhodamine derivatives, Biophys. J. 76 (1999) 469–477.
[26] R. Rizzuto, W. Carrington, R.A. Tuft, Digital imaging microscopy of living cells, Trends Cell Biol. 8 (1998) 288–292.
[27] E. Rapizzi, P. Pinton, G. Szabadkai, M.R. Wieckowski, G. Vandecasteele, G.S. Baird, R.A. Tuft, K.E. Fogarty, R. Rizzuto, Recombinant expression of the voltage-dependent anion channel enhances the transfer of Ca^{2+} microdomains to mitochondria, J. Cell Biol. 159 (2002) 613–624.
[28] R. Rizzuto, M. Brini, M. Murgia, T. Pozzan, Microdomains with high Ca^{2+} close to IP3-sensitive channels that are sensed by neighboring mitochondria, Science 262 (1993) 744–747.
[29] M. Montero, M. Brini, R. Marsault, J. Alvarez, R. Sitia, T. Pozzan, R. Rizzuto, Monitoring dynamic changes in free Ca^{2+} concentration in the endoplasmic reticulum of intact cells, EMBO J. 14 (1995) 5467–5475.
[30] M. Brini, D. Bano, S. Manni, R. Rizzuto, E. Carafoli, Effects of PMCA and SERCA pump overexpression on the kinetics of cell Ca^{2+} signalling, EMBO J. 19 (2000) 4926–4935.
[31] B. Landolfi, S. Curci, L. Debellis, T. Pozzan, A.M. Hofer, Ca^{2+} homeostasis in the agonist-sensitive internal store: functional interactions between mitochondria and the ER measured in situ in intact cells, J. Cell Biol. 142 (1998) 1235–1243.
[32] B.J. Marsh, D.N. Mastronarde, K.F. Buttle, K.E. Howell, J.R. McIntosh, Organellar relationships in the Golgi region of the pancreatic beta cell line, HIT-T15, visualized by high resolution electron tomography, Proc. Natl. Acad. Sci. USA 98 (2001) 2399–2406.
[33] Y. Kirichok, G. Krapivinsky, D.E. Clapham, The mitochondrial calcium uniporter is a highly selective ion channel, Nature 427 (2004) 360–364.
[34] M. Yi, D. Weaver, G. Hajnoczky, Control of mitochondrial motility and distribution by the calcium signal: a homeostatic circuit, J. Cell Biol. 167 (2004) 661–672.
[35] A. Varadi, V. Cirulli, G.A. Rutter, Mitochondrial localization as a determinant of capacitative Ca^{2+} entry in HeLa cells, Cell Calcium 36 (2004) 499–508.
[36] F. De Giorgi, L. Lartigue, F. Ichas, Electrical coupling and plasticity of the mitochondrial network, Cell Calcium 28 (2000) 365–370.
[37] S.S. Smaili, J.T. Russell, Permeability transition pore regulates both mitochondrial membrane potential and agonist-evoked Ca^{2+} signals in oligodendrocyte progenitors, Cell Calcium 26 (1999) 121–130.